

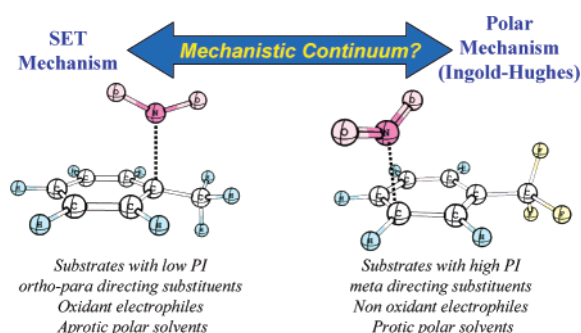
Electrophilic Aromatic Nitration: Understanding Its Mechanism and Substituent Effects[†]

Jorge Freire de Queiroz,[‡] José Walkimar de M. Carneiro,^{*,‡} Adão A. Sabino,[§]
Regina Sparrapan,[§] Marcos N. Eberlin,^{*,§} and Pierre M. Esteves^{*,||}

Instituto de Química, Universidade Federal Fluminense, Outeiro de São João Batista, s/n, 24020-150, Niterói-RJ, Brazil, Instituto de Química, Universidade Estadual de Campinas, Laboratório ThomSON de Espectrometria de Massas, Campinas, SP, Brazil, and Instituto de Química, Universidade Federal do Rio de Janeiro, Cidade Universitária, CT Bloco A, 21949-900, Rio de Janeiro-RJ, Brazil

walk@kabir.gqt.uff.br; eberlin@iqm.unicamp.br; pesteves@iq.ufrj.br

Received May 7, 2006



Theoretical calculations and gas-phase mass spectrometric studies were performed for the reaction of the naked (NO_2^+) and monosolvated ($\text{CH}_3\text{NO}_2 \cdot \text{NO}_2^+$) nitronium ion with several monosubstituted aromatic compounds. From these studies, we propose a general model for regioselectivity based on the single-electron transfer (SET) mechanism and an alternative mechanistic scheme for electrophilic aromatic nitration. This scheme considers the SET and the polar (Ingold–Hughes) mechanisms as extremes in a continuum pathway, the occurrence and extents of both mechanisms being governed mainly by the ability, or lack of ability, of the aromatic compound to transfer an electron to NO_2^+ .

Introduction

The mechanism of electrophilic aromatic nitration has been enthusiastically debated over decades.^{1–8} Ingold and Hughes considered the nitronium ion (NO_2^+) as the reactive electrophile

that attacks the aromatic compound (ArX) to form an ArXNO_2^+ intermediate.¹ This key intermediate is frequently referred to as the Wheland intermediate, σ complex, or arenium ion.² Subsequently, ArXNO_2^+ eliminates H^+ , and the neutral nitrated product is formed.³ This classical interpretation is known as the Ingold–Hughes or polar two-electron mechanism of electrophilic aromatic nitration. Kerner and Weiss also offered an alternative mechanism that assumes single-electron transfer (SET) from the aromatic substrate to NO_2^+ .⁴ Pair recombination of the two nascent SET products (the aromatic radical cation $\text{ArH}^{+\bullet}$ and the NO_2^\bullet radical) would then afford the same Ingold–Hughes arenium ion intermediate ArHNO_2^+ (Scheme 1).

[†] This manuscript is dedicated to Prof. W. B. Kover for his outstanding work on reaction mechanisms.

[‡] Universidade Federal Fluminense.

[§] Universidade Estadual de Campinas.

^{||} Universidade Federal do Rio de Janeiro.

(1) (a) Hughes, E. D.; Ingold, C. K.; Reed, R. I. *Nature* **1946**, *158*, 448. (b) Ingold, C. K.; Hughes, E. D. et al.; *J. Chem. Soc.* **1950**, 2400. (c) Ingold, C. K. *Structure and Mechanism in Organic Chemistry*; Cornell University Press: New York, 1969.

(2) (a) Wheland, G. W.; *J. Am. Chem. Soc.* **1942**, *64*, 900. (b) Wheland, G. W. *The Theory of Resonance*; Wiley: New York, 1944. (c) Olah, G. A. *Acc. Chem. Res.* **1971**, *4*, 240.

(3) Melander, L.; *Isotope Effects on Reaction Rates*; Ronald Press: New York, **1960**.

(4) (a) Kenner, J. *Nature*, **1945**, *156*, 369. (b) Weiss, J. *Trans. Faraday Soc.* **1946**, *42*, 116.

(5) Perrin, C. L. *J. Am. Chem. Soc.* **1977**, *99*, 5516.

(6) Ebersson, L.; Hartshorn, M. P.; Radner, F. *Acta Chem. Scand.* **1994**, *48*, 937.

(7) Olah, G. A.; Malhotra, R.; Narang, S. C. *Nitration Methods and Mechanism*; VCH: New York, 1989.

(8) Kochi, J. K. *Acc. Chem. Res.* **1992**, *25*, 39.

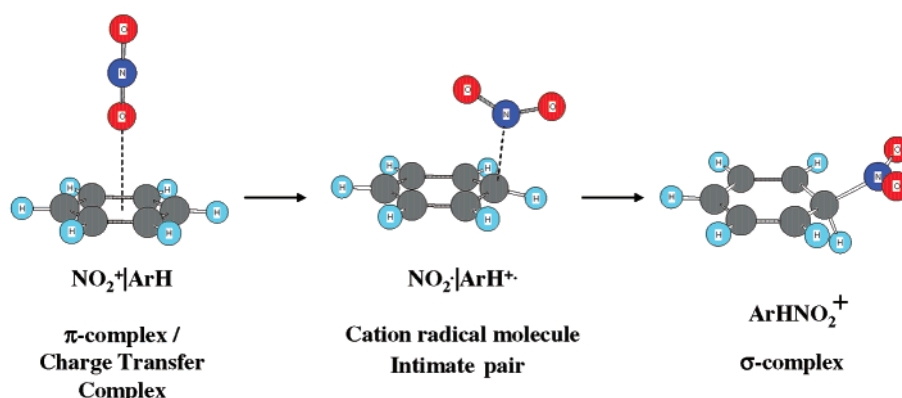
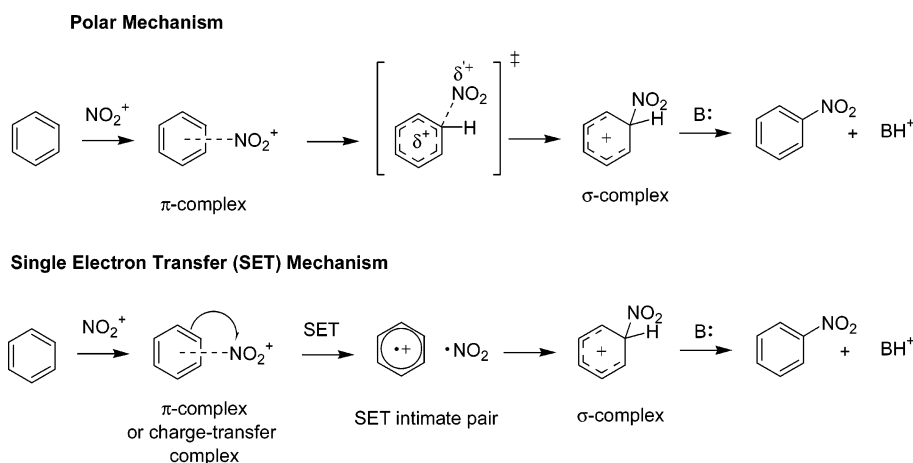


FIGURE 1. Key SET intermediates found by DFT calculations for nitration of benzene.

SCHEME 1



Although the Ingold–Hughes mechanism has prevailed, the SET mechanism has attracted renewed attention. A turning point occurred in 1977 when Perrin⁵ showed that electrochemical nitration of naphthalene yields the same proportion of products as that obtained on usual acidic nitration. Although Perrin's results were at first contested,⁶ they raised a vivid dispute on the validity and limits of the two mechanistic proposals.⁷ Kochi and co-workers⁸ offered considerable advance in clarifying the dispute by providing strong evidence for the SET mechanism based mainly on experimental results. They also formulated a slightly different SET mechanism in which more intermediates are involved. Nowadays, the SET mechanism seems to be firmly supported on an experimental base, particularly for the more activated (electron-rich) aromatics, hence coexisting on equal grounds (and therefore mixing up) with the Ingold–Hughes mechanism.

The first theoretical investigations reported on SET mechanism for electrophilic aromatic nitration were also controversial.⁹ However, high level theoretical investigations have corroborated the experimental findings pointing firmly to the SET mechanism.¹⁰ Recently, we¹¹ employed B3LYP/6-311++G(d,p) cal-

culations to show that gas-phase nitration of benzene with NO_2^+ involves first an electrostatically bonded π complex, which is better described as a charge-transfer complex (Figure 1), in which NO_2^+ interacts with the whole aromatic π system of benzene through one of its oxygen atoms. SET occurs within this initial π complex thus yielding a second complex, that is, a SET-intimate ion pair, which further collapses to the σ complex. Theoretical calculations¹² by other groups have also supported this model.

The proposal of a first π complex as an intermediate allowed us to rationalize some intriguing experimental findings from gas-phase ion/molecule reactions¹³ and in the condensed phase.¹⁴ For instance, it has been observed that, instead of the addition of NO_2^+ to benzene, the ion/molecule reaction between gaseous NO_2^+ and benzene occurs by oxygen atom transfer (formally O^+) to form $\text{C}_6\text{H}_6\text{O}^+$.¹⁵ On the basis of the SET mechanism, we have shown¹¹ that a phenol radical cation complexed to NO is the lowest energy species on the overall potential energy surface of $\text{C}_6\text{H}_6\text{NO}_2^+$. The loss of NO by this complex is the preferred pathway, affording the phenol radical cation ($\text{C}_6\text{H}_6\text{O}^+$).

(12) (a) Gwaltney, S. R.; Rosokha, S. V.; Head-Gordon, M.; Kochi, J. K. *J. Am. Chem. Soc.* **2003**, *125*, 3273. (b) Chen, L.; Xiao, H.; Xiao, J.; Gong, X. *J. Phys. Chem. A* **2003**, *107*, 11440.

(13) (a) Attinà, M.; Cacace, F.; Yanez, M. *J. Am. Chem. Soc.*, **1987**, *109*, 5092. (b) Aschi, M.; Attinà, M.; Cacace, F.; Ricci, A. *J. Am. Chem. Soc.* **1994**, *116*, 9535. (c) Attinà, M.; Cacace, F.; de Petris, G. *Angew. Chem., Int. Ed. Engl.* **1987**, *26*, 1177. (d) Cacace, F. *Acc. Chem. Res.* **1988**, *21*, 215.

(14) Olah, G. A.; Malhotra, R.; Narang, S. C. *Nitration Methods and Mechanism*; VCH: New York, 1989; Chapter 3.

(9) (a) Politzer, P.; Jayasuriya, K.; Sjöberg, P.; Laurence, P. R.; *J. Am. Chem. Soc.* **1985**, *107*, 1174. (b) Feng, J.; Zheng, Z.; Zerner, M. C.; *J. Org. Chem.* **1986**, *51*, 4531. (c) Gleghorn, J. T.; Torossian, G. *J. Chem. Soc., Perkin Trans. 2* **1987**, 1303.

(10) (a) Peluso, A.; Del Re, G.; *J. Phys. Chem.* **1996**, *100*, 5303. (b) Albuina, A. R.; Borrelli, R.; Peluso, A. *Theor. Chem. Acc.* **2000**, *104*, 218.

(11) Esteves, P. M.; Carneiro, J. W. d. M.; Cardoso, S. P.; Barbosa, A. G. H.; Laali, K. K.; Rasul, G.; Prakash, G. K. S.; Olah, G. A. *J. Am. Chem. Soc.* **2003**, *125*, 4836.

TABLE 1. B3LYP/6-311++G(d,p)//B3LYP/6-31++G(d,p) Relative Energies in Kcal Mol⁻¹ for the Minima Found for Species 1–4 (Scheme 2) Proposed for the Reaction of Gaseous NO₂⁺ with Selected Monosubstituted Aromatic Compounds via the SET Mechanism^a

species	X									
	NO ₂	CHO	CF ₃	CN	H	CH ₃	F	Cl	Br	OH
1	1 → 4	12.0 ^c	7.6 ^d	20.3	14.3 ^f	3.0 ^e	-3.4 ^c	-2.7 ^c	-3.5 ^c	-2.4 ^c
2a	17.3	2a → 2b	2.5	12.0	0.7 ^f	4.3	3.4	3.4	4.0	8.0
2b	15.4	18.8	0.0	11.2		4.2	4.4	4.1	3.5	2b → 3b
2c	15.7	18.0	0.5	12.3		6.7	2c → 2d	2c → 2d	2c → 3d	2c → 3d
2d	16.8	18.5	1.4	10.7		2d → 3d	1.3	1.6	1.4	2d → 3d
3a	3a → 2a	-17.6 ^b	8.1	3a → 2a		8.4	3a → 2a	3a → 2a	11.1	3a → 2a
3b	3b → 2b	20.6	3b → 2b	13.2		2.4	4.5	3.9	3.8	4.8
3c	17.7	18.0	1.5	14.5		5.8	8.4	8.3	8.5	16.8
3d	18.7	19.0	2.6	11.7	0.0 ^f	0.0	0.0	0.0	0.0	0.0
4	0.0	0.0	5.6	0.0			12.1	6.3	2.9	15.3

^a The blank fields mean that the structures could not be found as minima on the potential energy surface after geometry optimization. ^b **3a** rearranges to PhNO₂H⁺⋯CO upon geometry optimization. ^c Oxygen transfer to the ortho position. ^d Bent over the substituent, oxygen pointing toward ipso position. ^e Oxygen transfer to the ipso position. ^f From ref 11.

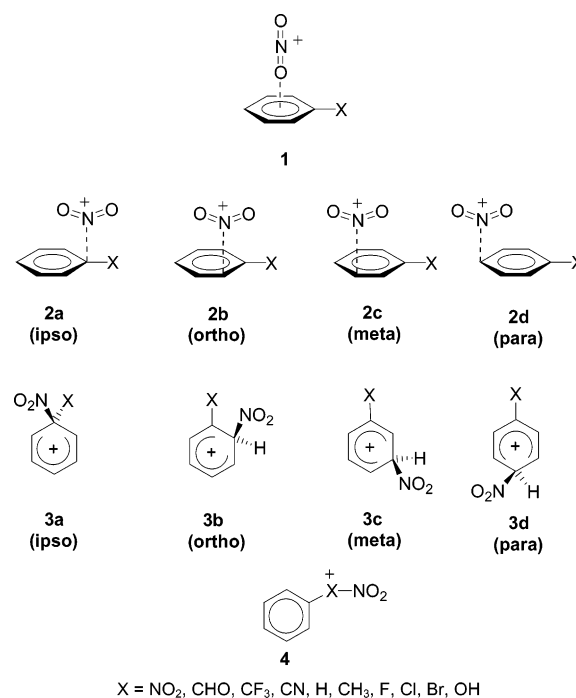
The reaction of the radical cation of several aromatics with NO₂ has been studied.¹⁶ The σ complex was readily formed for activated aromatics, whereas aromatics highly deactivated by multiple fluorine substitution were found to be nonreactive at all. Comparing these results with the lack of adduct formation in the reaction of aromatics with NO₂⁺ (as we show here however, monosolvated NO₂⁺ does add to aromatics), it was concluded that the ionized aromatic is a plausible intermediate in aromatic nitration. Speranza and co-workers¹⁷ used ICR experiments to show that SET is faster than ring nitration in the reaction of (RONO₂)H⁺ with aromatics, which eventually reacts with the precursor RONO₂ to afford oxygen transfer and nitration products. They also have shown that the direct oxygen and NO₂ group transfers from (RONO₂)H⁺ to the aromatic compound are slower than the single electron transfer. Therefore these experimental results,^{15–17} when analyzed in view of the SET mechanism,¹¹ are easily understood.

In an ongoing investigation aimed to fully understand the mechanism of electrophilic aromatic nitration, we report herein the results from a systematic experimental and theoretical study of the reaction of gaseous NO₂⁺ with monosubstituted aromatic compounds. These results are evaluated in view of substituent effects and considering both the SET and the Ingold–Hughes mechanism for electrophilic nitration reactions. From these studies, we propose a model for regioselectivity based on the SET mechanism and a general mechanistic scheme for electrophilic aromatic nitration conciliating, for the first time, the two coexisting views.

Results and Discussions

Theoretical Calculations on Key SET Species. The reaction of NO₂⁺ with selected aromatic compounds was initially studied by DFT using the B3LYP hybrid functional and the 6-311++G(d,p) basis set (6-31++G(d,p) for geometry optimization).¹⁸ Many possible orientations for the approximation of NO₂⁺ to

SCHEME 2



the aromatic compounds were considered (Scheme 2). See computational details for additional information.

Table 1 summarizes the relative energies for the main intermediates found on the potential energy surface for the interaction of NO₂⁺ with C₆H₅X (Scheme 2). Information on selected geometrical parameter and absolute energies, zero-point vibrational energy (ZPE), and thermal corrections to 298.15 K and 1 atm are provided as Supporting Information.

The potential energy surface for addition of NO₂⁺ to benzene is rather complex.¹¹ When unsymmetrical aromatic systems are considered, this complexity becomes even greater as compared to the symmetric benzene molecule. A wide set of minimum energy structures may be located, from which at least three are of primary relevance to the nitration mechanism. The first minimum is a weak π complex that represents a preorganized weakly bonded state, where low energy, nonspecific, and

(15) (a) Benezra, S. A.; Hoffman, M. K.; Bursey, M. M. *J. Am. Chem. Soc.* **1970**, *92*, 7501. (b) Hoffman, M. K.; Bursey, M. M. *Tetrahedron Lett.* **1971**, 2539. See also (c) Dunbar, R. C.; Shen, J.; Olah, G. A. *J. Am. Chem. Soc.* **1972**, *94*, 6862. (d) Ausloos, P.; Lias, S. G. *Int. J. Chem. Kinet.* **1978**, *10*, 657. (e) Morrison, J. D.; Stanney, K.; Tedder, J. M. *J. Chem. Soc., Perkin Trans. 2* **1981**, 967.

(16) (a) Schmitt, R. J.; Ross, D. S.; Buttrill, S. E. *J. Am. Chem. Soc.* **1981**, *103*, 5265. (b) Schmitt, R. J.; Buttrill, S. E.; Ross, D. S. *J. Am. Chem. Soc.* **1984**, *106*, 926.

(17) Attinà, M.; Cacace, F.; Speranza, M. *Int. J. Mass Spectrom. Ion Processes* **1992**, *117*, 37.

(18) (a) Hohenberg, P.; Kohn, W. *Phys. Rev.* **1964**, *136*, B864. (b) Kohn, W.; Sham, L. J. *Phys. Rev.* **1965**, *140*, A1133. (c) Parr, R. G.; Yang, W. *Density-Functional Theory of Atoms and Molecules*; Oxford University Press: Oxford, U.K. 1989.

attractive interaction between NO_2^+ and the aromatic π system as a whole occurs. This initial complex is followed by SET from the aromatic ring to NO_2^+ , resulting in an intimate ion-pair intermediate where a bent NO_2 molecule interacts with the benzene radical cation.¹¹ Collapse of the last intermediate affords the classical Wheland intermediate (σ complex).

Ring substituents should have therefore strong effects on the relative stability of the relevant intermediates. A major substituent effect is on the energy and structure of the unoriented π complex. For benzene (the parent aromatic compound), NO_2^+ is found to lay in the axis normal to the molecular plane of the aromatic ring with a stabilization energy of $-9.2 \text{ kcal mol}^{-1}$.¹¹ Similar arrangements were located only for the aromatics bearing the electron-withdrawing deactivating substituents CN and CF_3 . These substituents are known to decrease nitration rate, as compared to benzene, and direct nitration to the meta position. Additionally, for the NO_2 , CHO, CN, and CF_3 substituents, SET is endothermic¹¹ (vide Supporting Information, Table S10). For activating substituents (F, CH_3 , OH), SET is exothermic and the first π complex intermediate could not be located. During geometry optimization, even when using an input geometry that forced NO_2^+ into a linear arrangement lying in the same axis as that of the aromatic ring, the structure converges directly to the SET intimate ion-pair complex. Therefore, the SET energetics seems to represent the main parameter that determines whether the π complex will be formed, whereas benzene represents the borderline for the process. Deactivating substituents leads to endergonic SET, therefore forming the π complex. In contrast, for activated substituents with exergonic SET, this complex could not be located.

The geometry of the π complex for benzonitrile ($X = \text{CN}$) is similar to that calculated for benzene. In this complex, NO_2^+ places itself in an axis perpendicular to the molecular plane of the aromatic ring. The only uncommon structure is found for trifluoro-toluene, that is, when the benzene ring bears the highly electronegative substituent CF_3 . NO_2^+ is found to move toward the substituent, and in the optimized structure it is located quite near to the CF_3 group, possibly owing to a strong electrostatic interaction.

The π complex just discussed may be considered as a charge-transfer complex involving electrostatic interactions. Analysis of CHelpG charges on the NO_2 and on the ArX moieties shows that these complexes have most of the positive charge on the NO_2 group, corroborating its description as a π complex. From this initial complex, the reaction evolves to the intimate ion-pair complex, where a bent NO_2 interacts with the aromatic ring. Therefore, the clear-cut step is SET from the aromatic ring to NO_2^+ , either via the unoriented preorganized π complex or via a direct electron shift for those cases where SET is exergonic.

Table 1 shows that all deactivated compounds with meta-directing substituents ($X = \text{NO}_2$, CHO, CF_3 , CN) have structures of the type **2b** and **2c**; that is, complexes at ortho and meta positions are the most stable ones. This trend seems to be general for this series. SET is also endergonic in this series, in agreement with estimates from differences in experimental ionization energies (IE).¹¹ Conversely, activated aromatic compounds containing ortho/para directing substituents form σ complexes (**3**) that are more stable than **1** or **2**. Analysis of charge densities for **2** shows that its positive charge is located mainly on the aromatic ring, indicating that SET to NO_2^+ has already occurred.

Thus, **2** is constituted formally of a pair of the NO_2^\bullet radical and the radical cation of the aromatic molecule $\text{ArX}^{\bullet+}$. Therefore, structures **2** are better described as SET intimate pairs, as observed for the nitration of benzene.¹¹

Halogen-substituted aromatics are interesting substrates for nitration since they are deactivated (as compared to benzene), but substitution is directed to the ortho and para positions.¹⁹ Therefore halobenzenes behave as borderlines. The present calculations show that they behave similarly to the activated aromatics, once they present exothermic SET.

Gas-Phase Reactions of NO_2^+ . To gain further insight as to whether and when SET or Ingold–Hughes mechanism operates, we performed mass spectrometric experiments in which gas-phase reactions of the isolated NO_2^+ and some selected aromatics were investigated. A pentaquadrupole mass spectrometer (Q1q2Q3q4Q5) was used.²⁰ First, we have reacted “naked” NO_2^+ generated by 70 eV electron ionization (EI) of nitro-methane (CH_3NO_2). The ion was mass-selected by the first quadrupole filter (Q1) and then sent to react with the aromatic compound to the second quadrupole collision chamber (q4). The product ion mass spectrum was then recorded by scanning the third quadrupole filter (Q5). As the spectrum of Figure 2 exemplifies for benzene, “naked” NO_2^+ reacts with the aromatics predominantly by electron abstraction yielding exclusively ionized benzene of m/z 78. None of the expected adduct of m/z 124 (likely the Wheland intermediate) was observed. Probably because direct addition of NO_2^+ to benzene is strongly exothermic, the nascent product is too hot to survive when it is isolated in the gas phase. The minor product ion of m/z 66 indicates that oxygen atom transfer also occurs to form hot ionized phenol, which dissociates readily by CO loss to the $\text{C}_5\text{H}_6^{\bullet+}$ ion of m/z 66. CO loss is the major dissociation observed for ionized phenol under EI, and the $\text{C}_5\text{H}_6^{\bullet+}$ ion has been rationalized as the cyclopentadienyl cation formed via the cyclohexadienone intermediate.²¹ The formation of a $\text{C}_6\text{D}_6\text{O}^{\bullet+}$ product ion of m/z 100 (likely ionized phenol) in reactions of NO_2^+ with benzene-*d*6 has been reported.¹⁵

To quench the ion/molecule products and hence to reduce or suppress their “reaction-induced” dissociation, we performed the next reactions with a monosolvated NO_2^+ ion. As observed before for other monosolvated ions,²² the third body (solvent) removes part of the energy released in the course of the reaction thus favoring the observation of the intact adduct of NO_2^+ with aromatics and olefins. Self-chemical ionization (CI) of CH_3NO_2 was then used to form $\text{CH}_3\text{NO}_2\cdot\text{NO}_2^+$ of m/z 107.²³

Figure 3a shows the spectrum for the gas-phase reactions of $\text{CH}_3\text{NO}_2\cdot\text{NO}_2^+$ of m/z 107 with benzene. Now for the monosolvated ion, three major products are formed. The adduct with benzene of m/z 124 is clearly detected. The product ion of m/z

(19) March, J. *Advanced Organic Chemistry*; John Wiley & Sons: New York, 1985.

(20) Eberlin, M. N. *Mass Spectrom. Rev.* **1997**, *16*, 113.

(21) Beynon, J. H.; Lester, G. R.; Williams, A. E. *J. Chem. Phys.* **1959**, *63*, 1861.

(22) (a) Dunbar, R. C.; Shen, J.; Olah, G. A. *J. Am. Chem. Soc.* **1972**, *94*, 6862. (b) Cacace, F.; Attinà, M.; de Petris, G.; Speranza, M. *J. Am. Chem. Soc.* **1994**, *116*, 6413. (c) Meurer, E. C.; Cabrinì, L. G.; Gozzo, F. C.; Eberlin, M. N. *J. Mass Spectrom.* **2006**, *41*, 735–740.

(23) Higher degree of solvation of NO_2^+ by CH_3NO_2 was not observed, despite many attempts to increase pressure and reduce the kinetic energy of the ions inside the CI cell. This limitation is probably because of the way the NO_2^+ is solvated (see text), which obstructs a second CH_3NO_2 molecule to strongly interact with NO_2^+ .

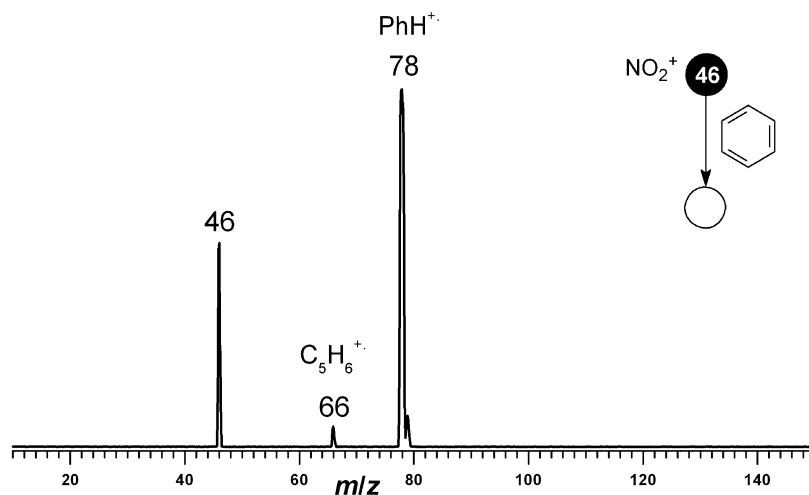


FIGURE 2. Product ion mass spectrum for the gas-phase reaction of naked NO_2^+ of m/z 46 with benzene (78 Da).

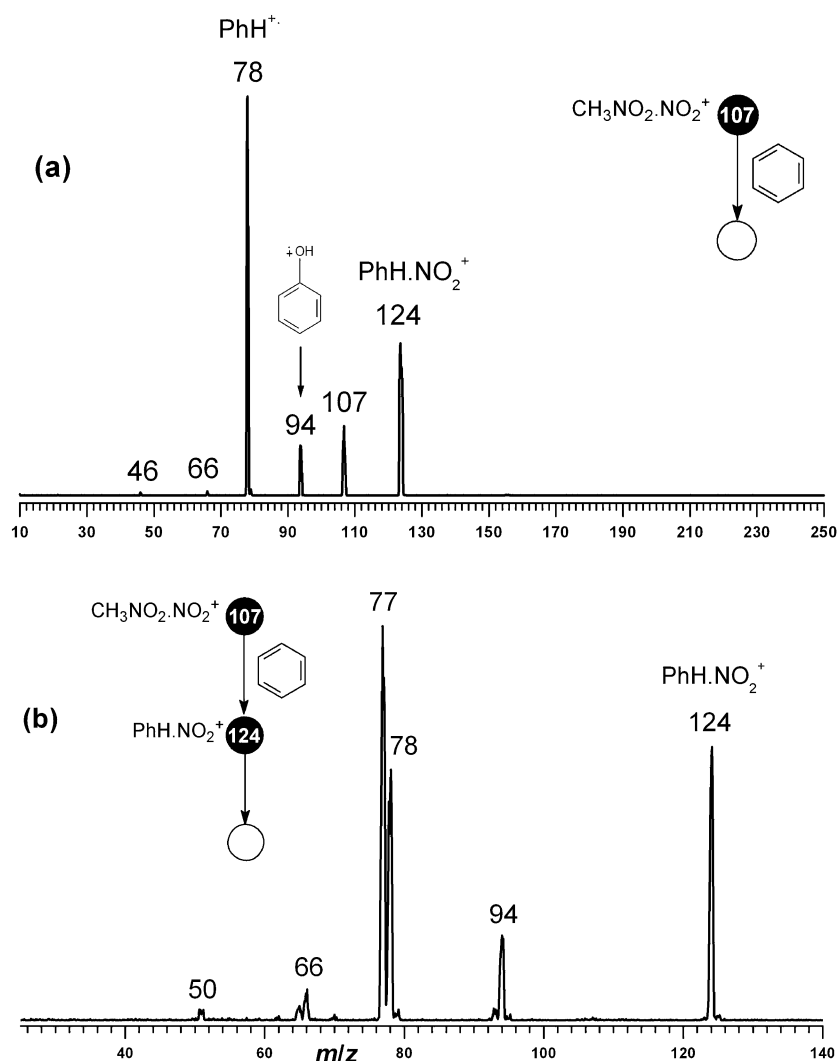


FIGURE 3. (a) Product ion mass spectrum for the gas-phase reaction of $\text{CH}_3\text{NO}_2\cdot\text{NO}_2^+$ of m/z 107 with benzene (78 Da). (b) Sequential product ion mass spectrum for 15 eV CID of the adduct of benzene and NO_2^+ of m/z 124.

94 is attributed to ionized phenol formed by oxygen atom ($\text{O}^{+\bullet}$) transfer, that is, by NO^\bullet loss from the intact adduct. The ion of m/z 78 is ionized benzene that can be accounted to be formed by SET if we consider that the gaseous intimate SET complex

is too hot and too weakly bonded to survive (no substantial heat removal from solvent) thus dissociating to ionized benzene and NO_2^\bullet before collapsing to the Wheland intermediate (the adduct).

SCHEME 3

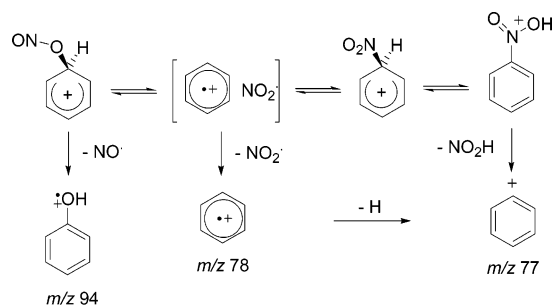


Figure 3b shows the sequential product ion mass spectrum for the adduct of benzene with NO_2^+ , that is $\text{PhH}\cdot\text{NO}_2^+$. The dissociation chemistry observed can be rationalized in terms of a mixture of coexisting or interconverting isomers (Scheme 3). The fragment of m/z 94 (likely ionized phenol formed by O^+ transfer)¹⁴ indicates dissociation of a species covalently bonded through the oxygen. The fragment of m/z 78 may be rationalized in terms of the Wheland intermediate that dissociates via the intermediacy of the intimate $\text{PhH}^+/\text{NO}_2^\bullet$ SET complex (Figure 1). The fragment of m/z 78 (ionized benzene, PhH^+) may then dissociate further by H loss to form Ph^+ of m/z 77, but this fragment may also be formed from the Wheland intermediate after proton shift.

Figure 4 shows now the spectra for the gas-phase reactions of $\text{CH}_3\text{NO}_2\cdot\text{NO}_2^+$ with toluene and anisole. If we consider the Ingold–Hughes mechanism, the increase of the nucleophilicity of the aromatic ring, as for toluene and anisole, would be expected to favor adduct formation. The SET mechanism would otherwise predict higher tendency of these electron-rich rings to transfer an electron to NO_2^+ . Lower yields for the $\text{PhX}\cdot\text{NO}_2^+$ adducts and higher yields of the ionized aromatics are observed, as compared to benzene (Figure 3a), and therefore these results are fully in line with the SET mechanism for nitration of aromatics.¹¹ In fact, anisole (Figure 4b) forms no $\text{PhOCH}_3\cdot\text{NO}_2^+$ adduct at all, and ionized anisole of m/z 108 dominates.

In great contrast to benzene and the activated aromatics (toluene and anisole), $\text{CH}_3\text{NO}_2\cdot\text{NO}_2^+$ reacts with the deactivated aromatic nitrobenzene forming the adduct $\text{PhNO}_2\cdot\text{NO}_2^+$ exclusively, with electron transfer ($\text{PhNO}_2^{\bullet+}$ of m/z 123) being entirely suppressed (Figure 5).

This contrasting behavior for activated and deactivated aromatics, for instance anisole (Figure 4b) and nitrobenzene (Figure 5), is therefore in opposition with the Ingold–Hughes mechanism, whereas it is fully consistent with the SET mechanism. The lower IE of the activated aromatics favor electron transfer (SET) as opposed to adduct formation, whereas the higher IE of nitrobenzene hampers electron-transfer thus favoring direct electrophilic attack with adduct formation (see Table S10, in the Supporting Information, for details).

Another tough test for the SET mechanism is offered by the reactions of $\text{CH}_3\text{NO}_2\cdot\text{NO}_2^+$ with the halobenzenes. In electrophilic aromatic substitution, the halogens Cl, Br, and I deactivate the aromatic ring but direct attack to the ortho/para positions. This classical dichotomy in aromatic substitution reactions has been explained by an imbalance between resonance (ortho/para orientation) and inductive effects (lower reactivity as compared to benzene).¹⁹

In full accordance with the SET mechanism, $\text{CH}_3\text{NO}_2\cdot\text{NO}_2^+$ reacts with the halobenzenes mainly by electron abstraction (Figure 6), whereas the lower the ionization energies ($\text{F} > \text{Cl}$

$> \text{Br} > \text{I}$)¹¹, the higher the yield of the ionized halobenzene as compared to that for the $\text{PhX}\cdot\text{NO}_2^+$ adduct. In fact, only fluorobenzene and chlorobenzene form detectable amounts of $\text{PhX}\cdot\text{NO}_2^+$ as well as the corresponding ionized halophenols,²⁴ whereas bromobenzene and iodobenzene afford only PhX^+ , probably as the result of their lowest IE within the halogen series (Table S10).

The key question that now rises is How can we predict how readily an aromatic ring can transfer a single electron to NO_2^+ ? The low feasibility of such process has been a main argument against the generalization of the SET mechanism for electrophilic aromatic nitration. This question may be addressed by inspection of the IE of the aromatics. Experimental IE measured in the gas phase are available²⁵ and provide an indication for the thermodynamic feasibility of the SET process.¹¹

SET to NO_2^+ from the parent aromatic compound benzene ($-7.89 \text{ kcal mol}^{-1}$) as well as from the activated aromatics toluene ($-17.48 \text{ kcal mol}^{-1}$), phenol ($-25.27 \text{ kcal mol}^{-1}$), anisole ($-31.96 \text{ kcal mol}^{-1}$), and aniline ($-43.03 \text{ kcal mol}^{-1}$) is thermodynamically favored (see table S10, for selected values). This favoring therefore increases as a function of the electron donating ability of the substituent.¹¹ SET for the deactivated and meta-orientating substituted aromatics nitrobenzene ($+8.16 \text{ kcal mol}^{-1}$), trifluorotoluene ($+2.28 \text{ kcal mol}^{-1}$), and benzonitrile ($+3.32 \text{ kcal mol}^{-1}$) are, as expected, unfavorable. Nevertheless, and again as observed experimentally, the deactivated and ortho/para orientating halobenzenes are predicted to undergo exothermic SET to NO_2^+ ($\Delta\text{IE} < 0$), in the order: $\text{F} (-8.90 \text{ kcal mol}^{-1}) > \text{Cl} (-11.9 \text{ kcal mol}^{-1}) > \text{Br} (-13.5 \text{ kcal mol}^{-1}) > \text{I} (-20.0 \text{ kcal mol}^{-1})$. The SET mechanism can also explain the observed ortho/para selectivity in the electrophilic nitration of halobenzenes, an unusual orientation for such deactivating groups (Figure 9, see *infra*). Care should be taken, however, to use gas-phase ΔIE since they provide only a rough prediction for solution behavior. This is so because solvent and counterion effects can change intrinsic IE, especially for the small NO_2^+ . Therefore, large gas-phase ΔIE are unlikely to be inverted by solution effects but inversions for small ΔIE may occur. If so, depending on the solvent and counterion, or both, nitration may follow either the SET or Ingold–Hughes mechanism, and a general model accounting for this behavior is discussed below. The SET mechanism can therefore be more evident in some solvents, especially in polar aprotic ones (Figure 7).

In aprotic polar media, such as nitromethane, the solvation of NO_2^+ is basically nucleophilic. Thus, its solvation occurs mainly at the positively charged nitrogen atom, which makes the N site less accessible for nucleophilic attack. This trend was observed in our gas-phase experiments, since NO_2^+ was unable to be monosolvated for more than one nitromethane molecule. The only related species observed in the self-ionization of CH_3NO_2 is the singly monosolvated NO_2^+ ($\text{CH}_3\text{NO}_2\cdot\text{NO}_2^+$ of m/z 107), despite all attempts to generate multisolvated species. If SET occurs in this scenario, the charges on the system change. On the NO_2 , now neutral because of SET, oxygen atoms bear the negative charge, whereas the nitrogen atom tends to be

(24) The product ion mass spectrum for CID of ionized fluorophenol of m/z 112 shows it dissociates mainly by CO loss.

(25) Linstrom P. J., Mallard, W. G., Eds. *NIST Chemistry WebBook*; NIST Standard Reference Database Number 69, March 2003; National Institute of Standards and Technology: Gaithersburg, MD, <http://webbook.nist.gov>. (See Supporting Information (Table S10) for summarized data from NIST.)

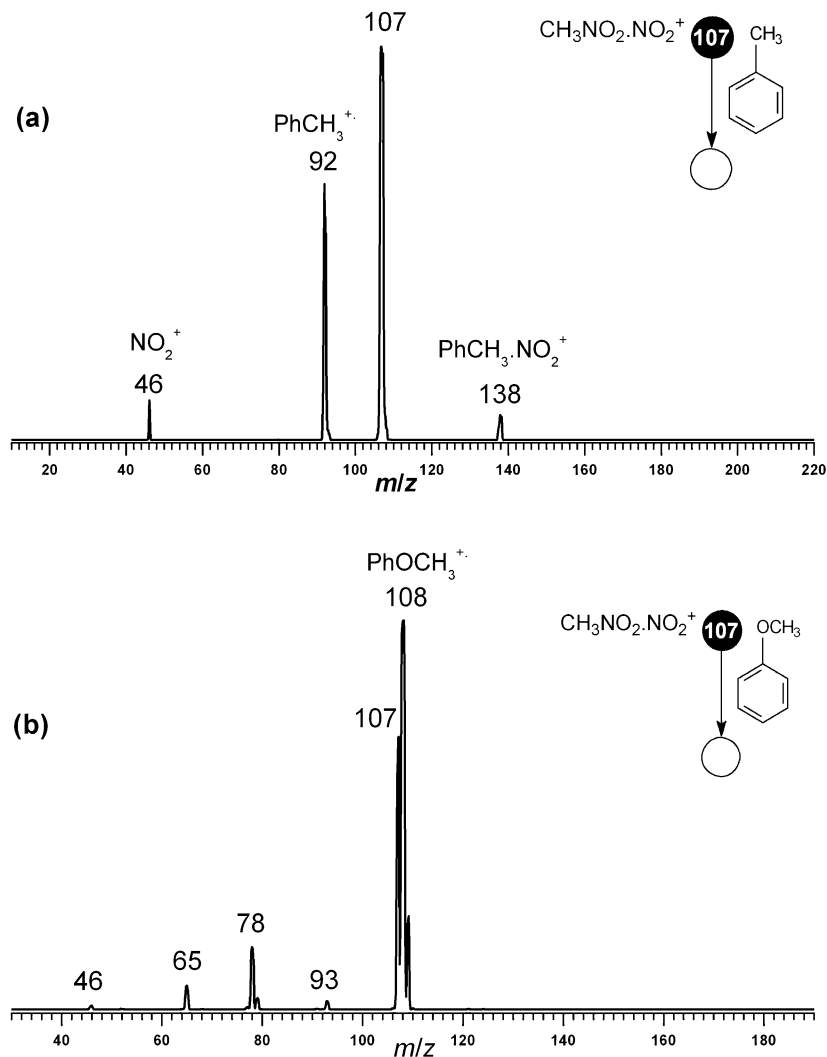


FIGURE 4. Product ion mass spectrum for the gas-phase reaction of $\text{CH}_3\text{NO}_2 \cdot \text{NO}_2^+$ of m/z 107 with (a) toluene (92 Da) and (b) anisole (108 Da).

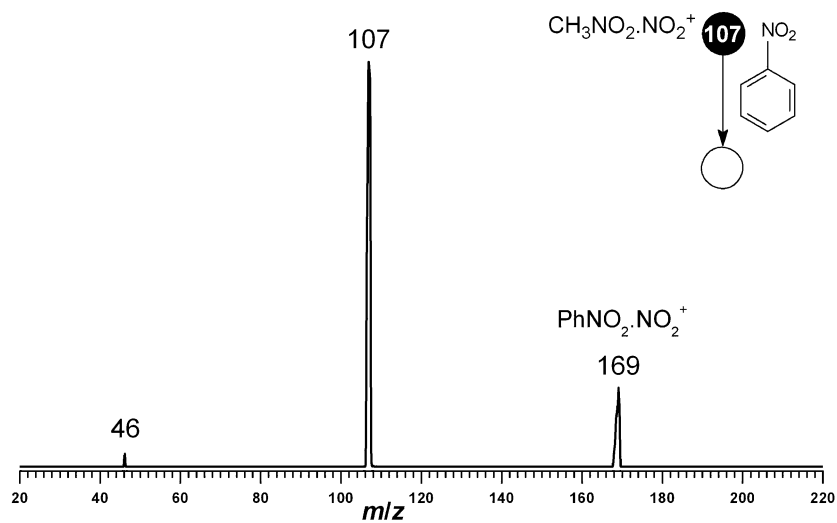


FIGURE 5. Product ion mass spectrum for the gas-phase reaction of $\text{CH}_3\text{NO}_2 \cdot \text{NO}_2^+$ of m/z 107 with nitrobenzene (123 Da).

neutral to positive. However, the aromatic is now a radical cation. There is greater tendency for an attack from the negatively charged oxygen atoms to the ring, leading to oxygen transfer products. This tendency explains the greater feasibility

of oxygen transfer in this case. Other reaction pathways are the coupling through the nitrogen atom, leading to the N-bonded Wheland intermediate, which will eventually afford the nitrated product. However, this pathway requires NO_2 rotation in the

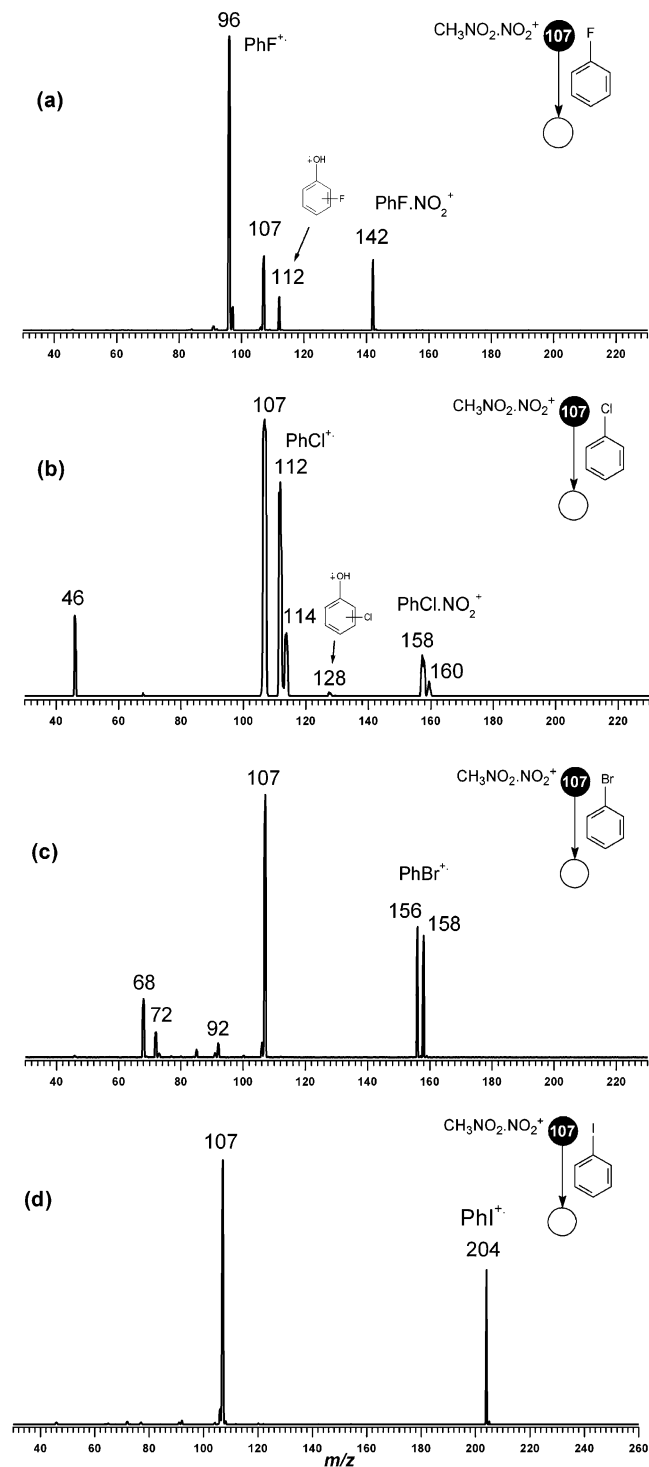


FIGURE 6. Product ion mass spectrum for the gas-phase reaction of $\text{CH}_3\text{NO}_2\cdot\text{NO}_2^+$ of m/z 107 with (a) fluorobenzene (96 Da), (b) chlorobenzene (112/114 Da), bromobenzene (156/158 Da), and (d) iodobenzene (204 Da).

SET intimate pair, which can also dissociate into NO_2 and the radical cation of the aromatic compound that could afford products from radical processes.

However, if polar protic solvents are considered, the solvation of NO_2^+ is both electrophilic and nucleophilic, respectively on the oxygen and nitrogen atoms. Upon SET, the partially negatively charged oxygen atoms on neutral NO_2 are even more

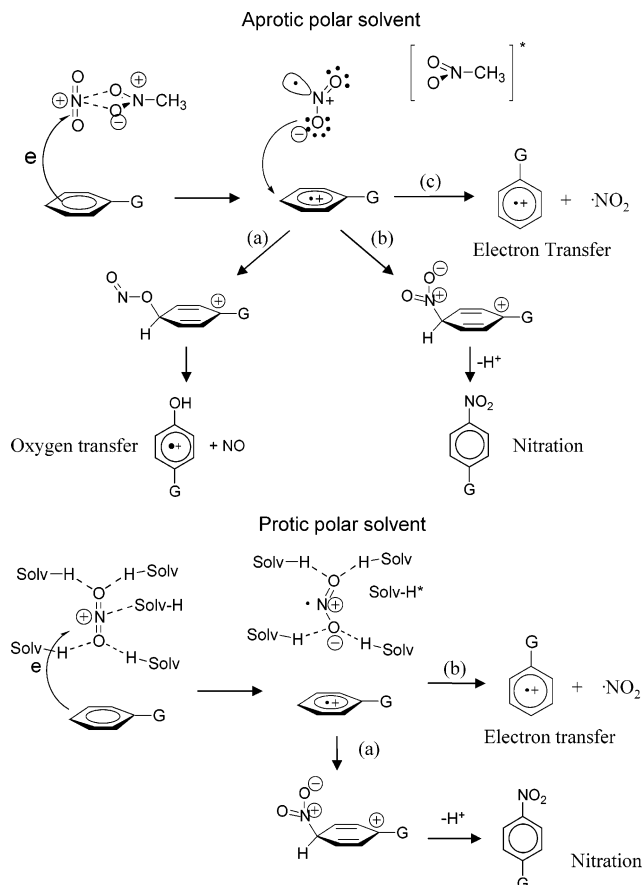


FIGURE 7. Mechanistic scheme proposed for the nitration of aromatics in aprotic (top) and protic (bottom) polar solvent. The asterisk sign (*) on a species means that it is vibrationally and translationally excited.

strongly solvated by hydrogen bonds from the media, whereas the nitrogen atom (in a radical) is relatively free of solvation for coupling with the radical cation of the aromatic compound. Thus, performing the reaction in polar protic or aprotic solvents can lead to different products and behavior, which could be the source for disagreement for the reaction mechanism.

A Frontier Molecular Orbital Model for SET. Analysis of the frontier molecular orbitals in terms of the donor–acceptor mechanism may help rationalize the role of the substituent on the reaction rate and regioselectivity observed in solution. The main interaction involves the highest occupied molecular orbital (HOMO) of the donor species, the aromatic compound in the present case, and the lowest unoccupied molecular orbital (LUMO) of the acceptor: NO_2^+ . Therefore, we need to understand how the substituent affects the orbital energies of the aromatic π system. Figure 8 shows a pictorial representation on the effect of substituents on the HOMO energies of the aromatic compound. Benzene has two degenerate HOMO orbitals, one of which is symmetric through mirroring whereas the other one is antisymmetric. Upon substitution by an electron donor substituent, Z, the degeneracy breaks down and the symmetric orbital became the higher energy (HOMO), because of the electron–electron repulsion of the electrons in the Z group with the aromatic π system. Conversely, upon substitution by an electron withdrawing group, Y, the symmetric orbital is stabilized, breaking down the degeneracy and leading the antisymmetric orbital to be the HOMO in this case.²⁶

(26) Fukuzumi, S.; Kochi, J. K.; *J. Am. Chem. Soc.* **1981**, *103*, 7240.

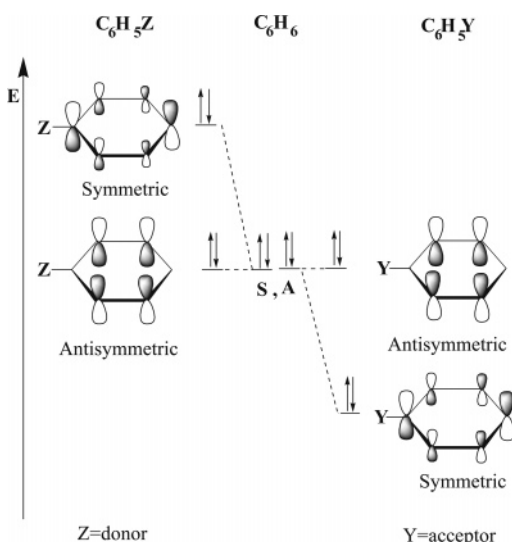


FIGURE 8. Substituent effects on the energy of frontier molecular orbitals of benzene.

Frontier MO energies found at the MP2(fc)/6-31G* level confirm the role of HOMO–LUMO interactions in governing substituent effects on electrophilic aromatic nitration. Table 2 shows the energies of HOMO, HOMO – 1, LUMO and LUMO + 1 for several monosubstituted aromatic compounds. Interaction between an electrophile/oxidant such as NO_2^+ and the aromatic compound should occur mainly in the positions containing the highest HOMO coefficients. Actually, the theoretical results indicate that the only minima found for electron-donor substituents, which actually correspond to SET intimate complex, are those where NO_2^+ is on the top of an ipso or para position. This arrangement is what is seen for the ipso and para complexes (Figure 9a and 9b). In contrast, aromatics containing electron-withdrawing substituents form complexes with NO_2^+ at the middle of the meta/ortho positions (Figure 9c).

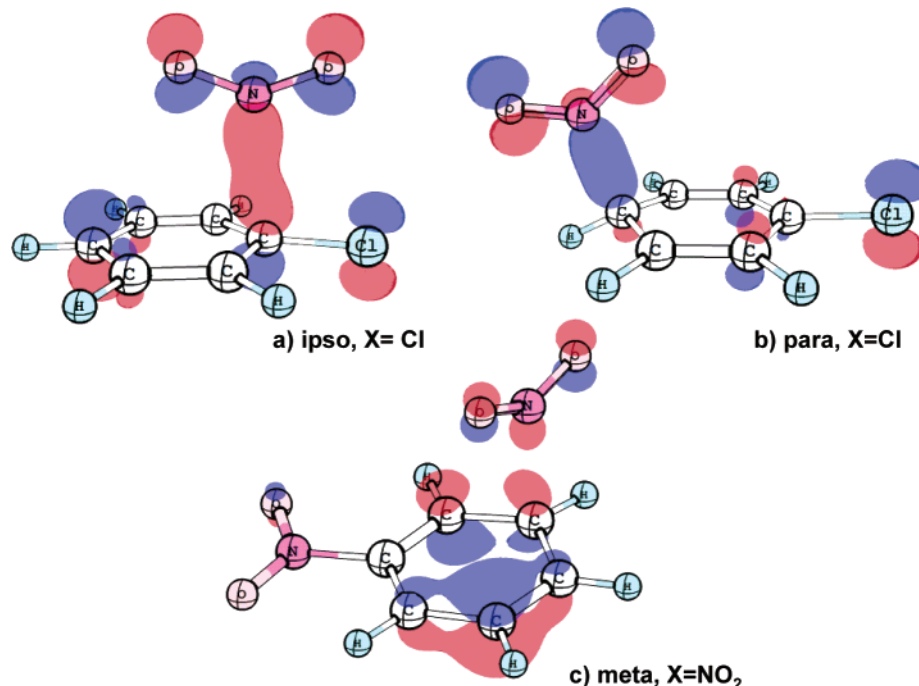
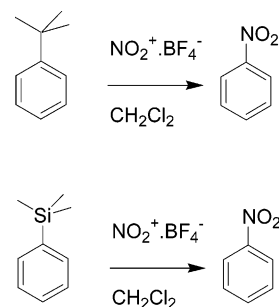


FIGURE 9. Frontier orbital interactions within complexes **2a** (a) and **2d** (b), for X = Cl, and **2c** (c), for X = NO_2 .

TABLE 2. MP2(fc)/6-31G(d)//MP2(fc)/6-31G(d) Energies of HOMO, HOMO – 1, LUMO and LUMO + 1 Orbitals in Hartrees for the Selected Aromatic Compounds as Well as for NO_2^+

substrate	HOMO	HOMO – 1	LUMO	LUMO + 1	ΔE (eV)
benzene	–0.329 (S)	–0.329 (A)	0.147 (A)	0.147 (S)	0.0
toluene	–0.317 (S)	–0.328 (A)	0.147 (A)	0.149 (S)	0.299
aniline	–0.290 (S)	–0.330 (A)	0.147 (A)	0.165 (S)	1.088
phenol	–0.310 (S)	–0.338 (A)	0.140 (A)	0.160 (S)	0.762
fluorobenzene	–0.334 (S)	–0.347 (A)	0.130 (A)	0.146 (S)	0.354
chlorobenzene	–0.333 (S)	–0.347 (A)	0.129 (S)	0.130 (A)	0.381
bromobenzene	–0.330 (S)	–0.348 (A)	0.126 (S)	0.129 (A)	0.490
nitrobenzene	–0.365 (A)	–0.374 (S)	0.046 (S)	0.113 (A)	0.245
benzaldehyde	–0.346 (A)	–0.350 (S)	0.078 (S)	0.130 (A)	0.109
trifluoromethylbenzene	–0.352 (A)	–0.357 (S)	0.112 (S)	0.125 (A)	0.136
NO_2^+	–0.920	–0.920	–0.264	–0.264	

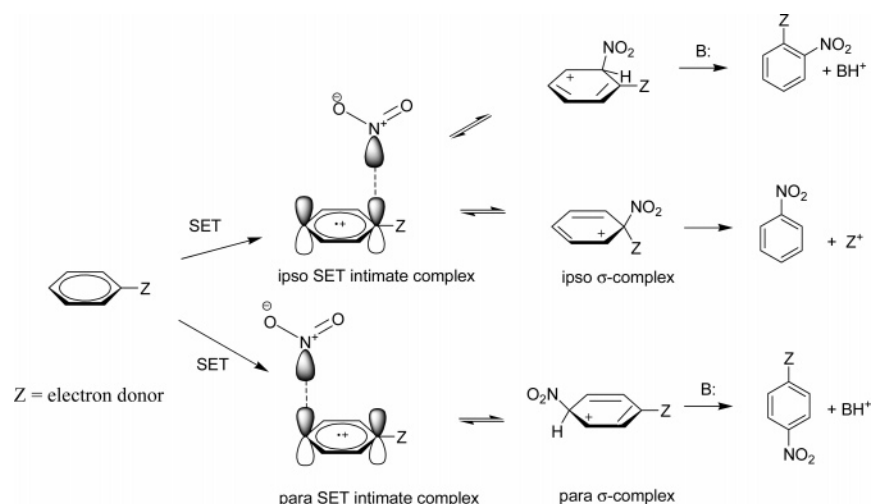
SCHEME 4



These HOMO–LUMO results together with the SET mechanism allow us to rationalize intriguing results in electrophilic aromatic nitrations,²⁷ such as the high degree of ipso substitution such as for the reactions summarized in Scheme 4.

When the substituent is a good leaving group, a SET intimate pair at the ipso position may be formed. Collapse of this complex to the Wheland intermediate at the ipso position followed by loss of the substituent affords the ipso substituted product. This mechanism likely operates, for example, for the

SCHEME 5



nitration of *tert*-butylbenzene and trimethylsilylbenzene (Scheme 4), which extensive nitration at the ipso position has been observed.²⁷ For monosubstituted aromatic compounds with meta-orientating deactivated substituents (X=CN, NO₂, CHO, CF₃), the SET to NO₂⁺ is unfavorable. Therefore, the interaction occurs between the HOMO of the aromatic compound and the LUMO of NO₂⁺. Since the HOMO of the aromatic compound has higher density on the atoms that have higher MO coefficients, a π complex should be formed with NO₂⁺ placed above the ortho and meta positions, as expected by MO analysis (Figure 8). Actually, this qualitative analysis is reinforced by our ab initio calculations. The evolution of the π complex (electron transfer is unfavorable) to the products involves the formation of a σ complex (Wheland intermediate), which will occur preferentially at the meta position, therefore minimizing the repulsion between positive charges, as suggested by the Ingold–Hughes mechanism.¹ We therefore propose, for electrophilic nitration of aromatics, that ortho/para substituent orientation, as well as the ipso substitution, is intimately related to the SET mechanism, whereas the meta substituent orientation is due to the Ingold–Hughes mechanism, given that SET cannot operate (endothermic).

SET usually involves avoided crossings into the electronic configurations (Figure 10). This avoided crossing happens at a geometry where degenerescence of one or more electronic configurations is necessary for correctly describing the electronic state of the system.²⁸ The geometry of the transition state for SET is therefore given by the geometry that leads to the avoided crossing in such systems. According to the Marcus theory, the energy needed to distort the geometry from its equilibrium position to the geometry where the configuration crossing occurs is given by the reorganization energy (λ).²⁹ For nitration, the main electronic reorganization is due to the geometrical distortion of NO₂⁺, once the aromatic compound presents little geometric (nuclei) reorganization for SET.^{6,11} Considering the

HOMO and LUMO energies and considering that these energies are good representations for the fundamental state, the analysis of the frontier MO allows us to roughly identify the point where SET occurs. This approach was successful for the analysis of nitration of benzene.¹¹

From the Marcus theory, the energy barrier for the electron transfer (E_a) may be approximately given by the sum of the reorganization energies of the aromatic compound (λ_{ArH^+}) and that of the electrophile ($\lambda_{\text{NO}_2^+}$). As commented above, the reorganization energy of the aromatic compound is rather small ($\lambda_{\text{ArH}^+} \sim 0$); therefore, this energy can be calculated by the following equation:

$$E = f(\lambda_{\text{ArH}^+} + \lambda_{\text{NO}_2^+}) \approx f(\lambda_{\text{NO}_2^+})$$

The energy barriers for SET involving several substituted benzenes can be estimated by looking for the ONO bond angle

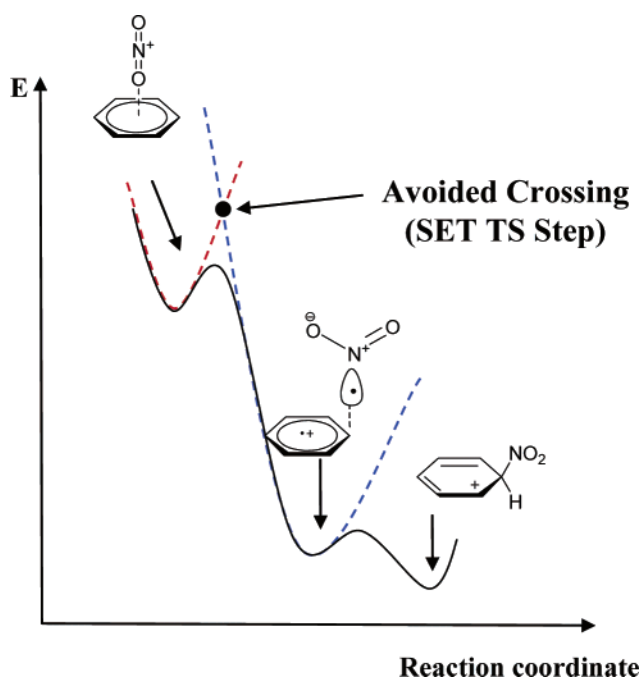


FIGURE 10. Avoided crossing on the nitration of benzene and its relation to the SET mechanism.

(27) (a) Olah, G. A.; Malhotra, R.; Narang, S. C. *Nitration Methods and Mechanism*; VCH: New York, 1989. (b) Perrin, C. L.; Skinner, G. A. *J. Am. Chem. Soc.* **1971**, *93*, 3389. (c) Nightingale, D. V. *Chem. Rev.* **1947**, *30*, 117. (d) Moodie, R. B.; Schofield, K. *Acc. Chem. Res.* **1976**, *9*, 287. (e) Attinà, M.; Cacace, F.; Ricci, A. *J. Phys. Chem.* **1996**, *100*, 4424.

(28) (a) Yarkony, D. R. *J. Phys. Chem.* **1996**, *100*, 18612–18628. (b) Pross, A. *Theoretical and Physical Principles of Organic Reactivity*; Wiley: New York, 1995.

(29) (a) Marcus, R. A. *Adv. Chem. Phys.* **1999**, *106*, 1. (b) Marcus, R. A. *J. Electroanal. Chem.* **2000**, *483*, 2.

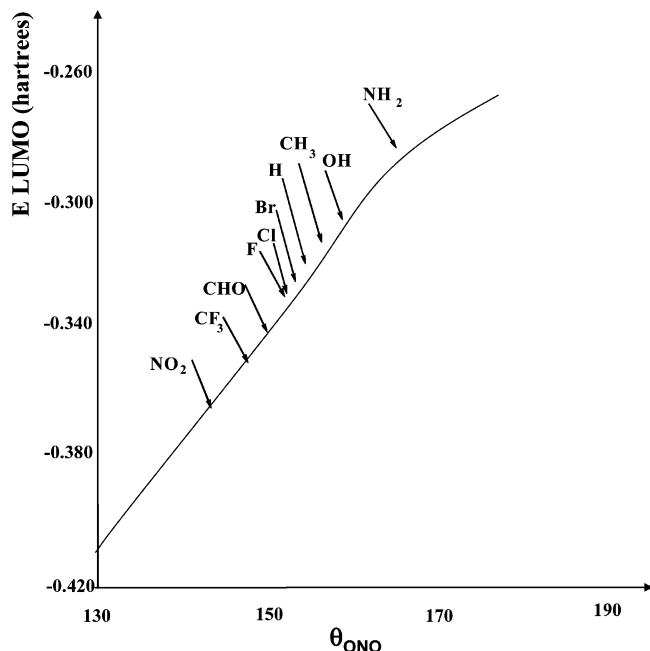


FIGURE 11. Plot of the LUMO energies of NO_2 versus θ_{ONO} . The arrows indicate the HOMO energies for the substituted $\text{C}_6\text{H}_5\text{X}$.

TABLE 3. Bending Angles of NO_2^+ Where Its LUMO Is Isoenergetic to the HOMO of the Aromatic Substrate

substituent (X)	ONO bond angle	bending energy of NO_2^+ (kcal mol^{-1})
NO_2	144°	22.3
CF_3	148°	18.0
CHO	150°	15.3
F, Cl	153°	13.0
Br	154°	12.0
H	155°	11.3
CH_3	158°	8.7
OH	160°	6.0
NH_2	167°	3.3

that affords the LUMO of NO_2^+ (Figure 11) isoenergetic to the HOMO of the aromatic.¹¹ MO analysis of NO_2^+ indicates that its LUMO, initially a degenerate one, becomes lower in energy as the ONO bond angle decreases, whereby resonance stabilization involving the nonbonded electron pairs on the oxygen atoms decreases.¹¹ For some ONO angles, the NO_2^+ LUMO should become isoenergetic to the HOMO of the aromatic, therefore making SET possible. We must know therefore the energy needed to bend the NO_2^+ geometry to an angle where the $\text{LUMO}_{\text{NO}_2^+}$ energy is equal to the HOMO_{ArH} energy. This energy represents an upper limit for the activation energy, since we are not considering the coupling of configurations, which decreases the energy of the electronic state.²⁸

Table 3 gives the energies needed to distort the NO_2^+ geometry so that its LUMO becomes isoenergetic to the HOMO of the interacting aromatic compound ($(\lambda_{\text{NO}_2^+})_{\text{X}}$). It may be observed beforehand that as the aromatic compounds are more activated for electrophilic aromatic substitution, their HOMO energies become higher. Thus, SET also becomes more favored, since the electronic reorganization energy in NO_2^+ necessary to make its LUMO isoenergetic with these higher HOMO energies is also smaller (Figure 11). For the more deactivated aromatics, such as nitrobenzene, for SET to become operational, the geometry of NO_2^+ should strongly change, resulting

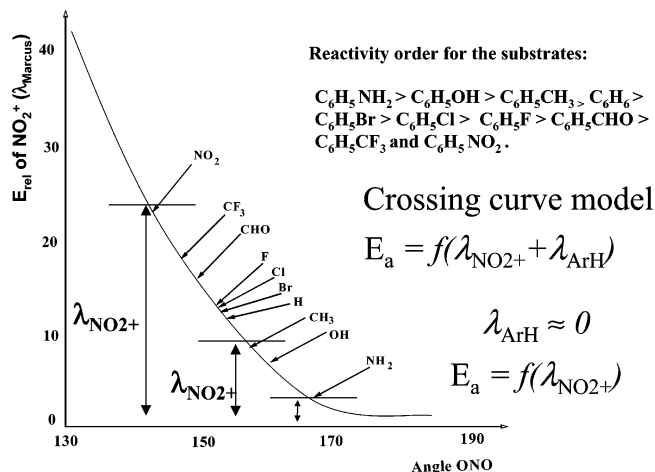


FIGURE 12. Plot of the relative energy (kcal mol^{-1}) of bent NO_2^+ in relation to the linear form versus ONO bond angles.

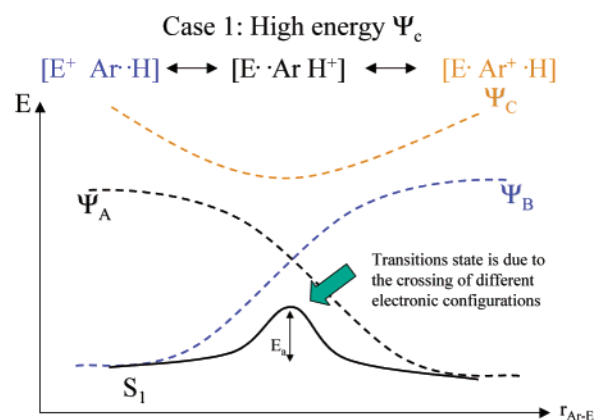


FIGURE 13. Avoided crossings and its relation to the state formation; high energy SET configuration.

thereafter in higher reorganization energy. As this reorganization energy increases, SET becomes less favorable, thus the deactivated compounds will react according to the polar Ingold–Hughes mechanism.

The analysis of the reaction profile using the avoided crossing model for electronic configurations and considering the SET paradigm, allows us to predict successfully the observed reactivity order for monosubstituted benzenes (Figure 12). SET steps are favored by substituents which increases the energy level of the HOMO of the aromatic. For higher energy HOMO in the aromatics, the reorganization energy needed to lower the energy of the LUMO of NO_2^+ (energy for bending the ONO bond angle) should be correspondingly lower. This criterion explains why electron-donating substituents such as CH_3 , OH, and NH_2 lead to activated aromatics with low activation energy, the contrary being observed for electron-attracting substituents.

For a general analysis of the electrophilic aromatic substitution we need to estimate whether the SET configuration is favored. Most probably, the mechanism of electrophilic aromatic substitution may be represented by a continuum pathway, where the SET and the Ingold–Hughes mechanisms are the extremes. For systems with SET configurations of high energy (see Figure 13), we should expect the reaction to occur through the polar Ingold–Hughes mechanism. However, if low energy SET configurations are allowed (Figure 14), more intermediates are

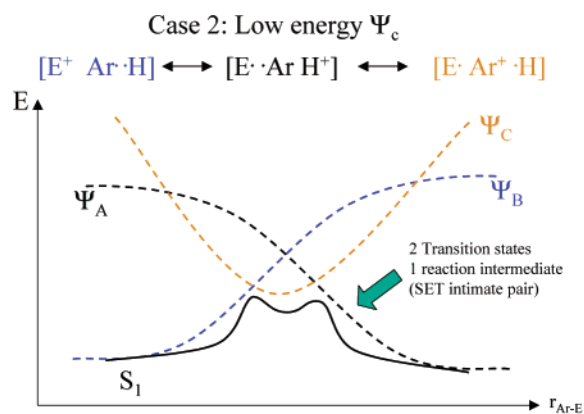


FIGURE 14. Avoided crossings and its relation with the state formation; low energy SET configuration, leading to the formation of an SET intimate pair as an intermediate.

expected, and the process should proceed preferentially by the SET pathway. For such situations, the intimate SET complex ($\text{ArH}^+\cdot/\text{NO}_2$) may be intercepted.

Conclusions

On the basis of the present theoretical calculations and gas-phase ion/molecule experiments, we propose an alternative and detailed mechanistic scheme for electrophilic aromatic nitration. This scheme consists of a continuum pathway in which the SET and the classical polar Ingold–Hughes mechanism represent extremes, and the prevalence of either one of these competing mechanisms depends on whether the aromatic compound is capable to transfer an electron to NO_2^+ . The operating mechanism, SET or Ingold–Hughes, is proposed to govern regioselectivity of substituents. The ortho/para directing groups conduct the reaction through the SET mechanism, while the meta directing groups favor the classic polar Ingold–Hughes mechanism.

Experimental and Computational Details

The geometry of several species was optimized using standard techniques, and, after geometry optimization, vibrational analysis was performed. The resulting geometries were checked with respect of being true minima on the potential energy surface, shown by the absence of any imaginary frequencies. Calculations were performed at B3LYP/6-311++G**//B3LYP/6-31++G** for all structures. All differences in energy refer to enthalpy differences, that is, zero-point energy and thermal expansion to 298 K corrections are taken into account besides the electronic energy. For frontier molecular orbital analysis, single point energy calculations at the MP2(fc)/6-31G**//B3LYP/6-31++G** level were performed. All calculations were performed with the Gaussian 98 package of programs.³⁰

The MS^2 and MS^3 experiments³¹ were performed using a pentaquadrupole (QqQqQ) mass spectrometer.³² The QqQqQ

consists of three mass-analyzing quadrupoles (Q1, Q3, Q5), in which ion mass-selection and mass-analysis are performed, and two radio frequency-only reaction quadrupoles (q2, q4). Reactions were then performed in q2 with selected aromatic compounds. For the MS^2 experiments, NO_2^+ of m/z 86 was generated by dissociative 70 eV electron ionization (EI) of nitromethane, whereas $\text{CH}_3\text{NO}_2\cdot\text{NO}_2^+$ was generated by self-chemical ionization of nitromethane. The reactant ion was then mass-selected by Q1, and after its ion/molecule reactions in q2 with the neutral reagents, Q5 was used to record the product ion mass spectrum, while operating Q3 and q4 in the “full” ion-transmission rf-only mode.

For the MS^3 experiments, a product ion of interest was mass-selected in Q3 and dissociated in q4 by collisions with argon, while Q5 was scanned across the desired m/z range to record the sequential product triple stage (MS^3) mass spectra. Nominal sample and neutral gas pressures were typically 5×10^{-6} and 5×10^{-5} Torr, respectively, as monitored by a single ionization gauge located centrally in the vacuum chamber. The target gas pressure corresponds to a typical beam attenuation of 50–70%, viz., to multiple collision conditions.^{33,34} However, lower reaction yields but similar sets of products were always observed at lower pressure, mainly single collision conditions in q2. Instrument parameters such as quadrupole offset potentials and lens voltages were adjusted to maximize the abundance of the ion/molecule reaction products. The collision energies, calculated as the voltages difference between the ions source and the collision quadrupole, were typically near 1 eV for ion–molecule reactions and 15 eV for CID.

Acknowledgment. Authors thank the Brazilian science foundations CNPq, FINEP-MCT, FAPERJ, and FAPESP for financial support.

Supporting Information Available: Tables containing total energies, zero-point energies (ZPE), thermal corrections and Cartesian coordinates of the species 1–4 and other species of interest; gas-phase IE for aromatic compounds and ΔIE for their reactions with NO_2^+ ; figures of the structures of interest containing selected bond lengths at their optimized geometries. This material is available free of charge via the Internet at <http://pubs.acs.org>.

JO0609475

(30) Lowry, T. H.; Richardson, K. S. *Mechanism and Theory in Organic Chemistry*; Harper and Row: New York, 1987, p 52.

(31) Frisch, M. J.; Trucks, G. W.; Schlegel, H. B.; Scuseria, G. E.; Robb, M. A.; Cheeseman, J. R.; Zakrzewski, V. G.; Montgomery, J. A., Jr.; Stratmann, R. E.; Burant, J. C.; Dapprich, S.; Millam, J. M.; Daniels, A. D.; Kudin, K. N.; Strain, M. C.; Farkas, O.; Tomasi, J.; Barone, V.; Cossi, M.; Cammi, R.; Mennucci, B.; Pomelli, C.; Adamo, C.; Clifford, S.; Ochterski, J.; Petersson, G. A.; Ayala, P. Y.; Cui, Q.; Morokuma, K.; Malick, D. K.; Rabuck, A. D.; Raghavachari, K.; Foresman, J. B.; Cioslowski, J.; Ortiz, J. V.; Stefanov, B. B.; Liu, G.; Liashenko, A.; Piskorz, P.; Komaromi, I.; Gomperts, R.; Martin, R. L.; Fox, D. J.; Keith, T.; Al-Laham, M. A.; Peng, C. Y.; Nanayakkara, A.; Gonzalez, C.; Challacombe, M.; Gill, P. M. W.; Johnson, B. G.; Chen, W.; Wong, M. W.; Andres, J. L.; Head-Gordon, M.; Replogle, E. S.; Pople, J. A. *Gaussian 98*, revision A.7; Gaussian, Inc.: Pittsburgh, PA, 1998.

(32) Eberlin, M. N. *Mass Spectrom. Rev.* **1997**, *16*, 113.

(33) Juliano, v. F.; Gozzo, F. C.; Eberlin, M. N.; Kascheres, C.; Lago, C. L. *Anal. Chem.* **1996**, *68*, 1328.

(34) Sparrapan, R.; Mendes, M. A.; Carvalho, M.; Eberlin, M. N. *Chem.—Eur. J.* **2000**, *6*, 321.